Chemical Science

ROYAL SOCIETY OF CHEMISTRY

EDGE ARTICLE

View Article Online
View Journal | View Issue

Cite this: *Chem. Sci.*, 2020, **11**, 11509

All publication charges for this article have been paid for by the Royal Society of Chemistry

A hierarchical assembly strategy for near-infrared photothermal conversion: unconventional heterogeneous metalla[2]catenanes†‡

Ye Lu, * Dong Liu, Yue-Jian Lin and Guo-Xin Jin *

Received 18th August 2020
Accepted 19th September 2020

DOI: 10.1039/d0sc04523c

rsc.li/chemical-science

Herein, we report a hierarchical assembly strategy for constructing heterogeneous half-sandwich organometallic D–A (D = π-donor, A = π-acceptor) interlocked structures, and their application in near-infrared (NIR) photothermal conversion. Thienothiophene and diketopyrrolopyrrole groups were selected as the D and A units, leading to two homogeneous metalla[2]catenanes with D–D–D–D and A–A–A–A stacks, respectively. By the ordered secondary assembly of homogeneous metalla[2]catenanes, two unprecedented heterogeneous D–A metalla[2]catenanes comprising an unusual mixed D–A–D–D and unconventional D–A–A–A stacks were realized by the combination of multiple noncovalent interactions, as all demonstrated by a detailed X-ray crystallographic study. Benefiting from the mixed D–A stacking modes, NIR absorption of heterogeneous D–A metalla[2]catenanes is significantly enhanced in contrast to homogeneous metalla[2]catenanes. Thanks to the enhanced NIR absorption and the fluorescence quenching effect from half-sandwich organometallic fragments, heterogeneous D–A metalla[2]catenanes displayed high-performance NIR photothermal conversion properties (η = 27.3%).

Introduction

Research into mechanically interlocked molecules, such as catenanes, rotaxanes, and molecular knots, has been gaining momentum in recent decades.[1] Electrostatic interactions between electron-rich (π-donor, D) and electron-poor (π-acceptor, A) aromatics are an important driving force in the self-assembly of interlocked structures.[2] Conventional wisdom and the current understanding of D–A interactions have thus far led to most of these catenanes being designed and synthesized with the (presumably most favorable) alternating parallel arrangement of π-rich and π-deficient units, providing D–A–D–A stacks in the final structure of organic [2]catenanes.[3] However, the advent of dynamic combinatorial libraries, presented by Sanders *et al.*, provided access to a larger variety of organic unusual donor–acceptor [2]catenanes, such as D–A–D–D, A–D–D–A, D–A–A–D or A–A–D–A stacks.[4] Metalla[2]catenanes based on coordination-driven self-assembly have long been limited to combinations of identical organometallic macrocycles or rectangles, which lead to symmetrical D–D–D–D or A–A–A–A stacks.[5] The high-yield preparation of some unconventional [2]catenanes, *e.g.* those based on unconventional D–A–A–A stacks, is extremely challenging even beyond the field of coordination-driven self-assembly.

Functional organic materials capable of photothermal conversion, *i.e.* that generate heat from infrared light, have attracted significant interest since the initial demonstrations of their application in a number of fields, especially on photothermal therapy and photothermal/photoacoustic imaging.[6] In order to pursue more high-performance photothermal conversion materials, extensive efforts are paid from two aspects: one is to enhance near-infrared (NIR) or infrared absorption through extending the molecular conjugation or linking D and A fragments; the other is to inhibit the radiative transition process by enhancing the quenching effect.[7] In fact, heterogeneous D–A metalla[2]catenanes based on half-sandwich organometallic Cp*Rh (Cp* = pentamethyl-cyclopentadienyl) fragments probably could reach these two aims at the same time. D and A units can be linked together by coordination bond of D–A metalla[2]catenanes and lead to alternating parallel arrangement.[8] Meantime, Cp*Rh fragments have inherent ability to quench fluorescence.[9]

Herein, we present a hierarchical self-assembly strategy for constructing heterogeneous organometallic D–A interlocked structures based on Cp*Rh fragments. We selected thienothiophene and diketopyrrolopyrrole groups as the D and A units, leading to two homogeneous metalla[2]catenanes with D–D–D–D and A–A–A–A stacks, respectively. By the ordered secondary assembly of homogeneous metalla[2]catenanes, two

State Key Laboratory of Molecular Engineering of Polymers, Shanghai Key Laboratory of Molecular Catalysis and Innovative Materials, Department of Chemistry, Fudan University, 2005 Songhu road, Shanghai, 200438, P. R. China

† Dedicated to Prof. Dr Pierre Dixneuf for his outstanding contribution to organometallic chemistry and catalysis.

‡ Electronic supplementary information (ESI) available. CCDC 1946051 (**Homo-1**), 1946991 (**Homo-2**), 1946053 (**Hetero-3**), 1946054 (**Hetero-4**). For ESI and crystallographic data in CIF or other electronic format see DOI: 10.1039/d0sc04523c

unprecedented heterogeneous D–A metalla[2]catenanes comprising unusual mixed D–A–D–D and D–A–A–A stacks were realized by the combination of multiple noncovalent interactions. Benefiting from the mixed D–A stacking modes and strong D–A interaction, heterogeneous D–A metalla[2]catenanes displayed stronger NIR absorption than homogeneous metalla[2]catenanes. We further took advantage of the enhanced NIR absorption to realize NIR photothermal conversion based on heterogeneous D–A metalla[2]catenanes.

Results and discussion

Homogeneous [2]catenanes

Diketopyrrolopyrrole groups, strong A units, have been widely applied in NIR organic optical materials.[10] Thus, their incorporation into metallarectangles could potentially lead to strong D–A interactions. Following this logic, D–A heterogeneous metalla[2]catenanes may can be obtained by ordered self-assembly between a metallarectangle based on D units and another metallarectangle based on A units, namely so-called hierarchical self-assembly strategy.[11] Hierarchical self-assembly is a multilevel and multistep self-assembly process that involves initial assembly of elementary molecular units into ordered secondary structures by noncovalent interactions, which has been used for the preparation of soft-matter nanoarchitectures and mechanically-interlocked M_8L_{16} container.[12] Hence, we initially prepared two types of metallarectangle, one based on D units, and the other based on A units. Thienothiophene groups were selected as strong D units to act as counterparts of the diketopyrrolopyrrole groups, in the form of the donor-containing pyridyl ligand **L1** (**L1** = 3,6-di(pyridin-4-yl) thieno[3,2-*b*]thiophene). We also designed another pyridyl ligand based on the diketopyrrolopyrrole A unit, namely **L2** (3,6-di(pyridin-4-yl)-2,5-dihydropyrrolo[3,4-*c*]pyrrole-1,4-dione). The geometrical configurations of **L1** and **L2** are very similar, apart from their electron rich and poor natures, respectively (Fig. 1a).

The next step was to prepare the individual D and A metallarectangles. We chose the precursor **P** (based on 2,5-dihydroxy-1,4-benzoquinoneas) as the binuclear precursor in this work as its metal–metal distance is *ca.* 7.9 Å, close to twice the conventional distance of π–π stacking (7 Å) (Fig. 1a).[13] Thanks to the optimized geometry and distance, a homo-[2]-catenanes (**Homo-1**) was obtained by the reaction of **P** and pyridyl ligand **L1** in methanol, which was confirmed by single-crystal X-ray crystallographic analysis and ESI-MS (Fig. 1b and S28‡). The four planes of the bithienyl solution, groups are nearly parallel to each other and the assembly comprises a D–D–D–D stack (red in Fig. 1b). There is an equilibrium between homo-[2]catenanes **Homo-1** and corresponding monomeric rectangle (MR) **1** in methanol solution. Upon dilution, the interlocked **Homo-1** transforms to MR **1**, which was further confirmed by ESI-MS, ^{1}H, ^{13}C, ^{1}H–^{1}H COSY and DOSY NMR spectroscopy (Scheme S1, Fig. S1–S8 and S29‡). **Homo-2** were also obtained by the reaction of **P** and **L2** in methanol solution, which was confirmed by single-crystal X-ray crystallographic analysis and ESI-MS (Fig. 1c and S30‡). The planes of the four electron-deficient units are also nearly parallel to each other, comprising an A–A–A–A stack (blue in Fig. 1c). Similar to **Homo-1**, the interlocked **Homo-2** transforms to corresponding MR **2** upon dilution, which was proven by ESI-MS ^{1}H, ^{13}C, ^{1}H–^{1}H COSY and DOSY NMR spectroscopy (Scheme S1, Fig. S9–S16 and S31‡).

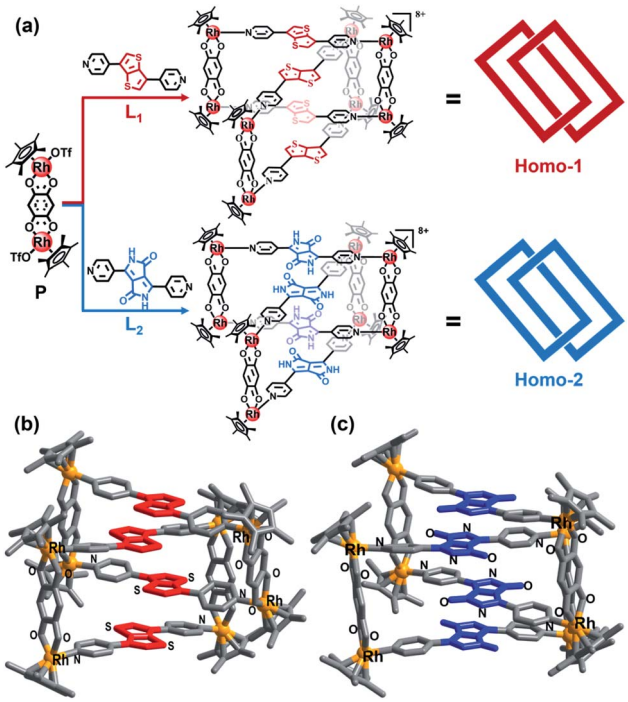

Fig. 1 (a) The synthesis of homogeneous metalla[2]catenanes; single-crystal X-ray structures of **Homo-1** (b) and **Homo-2** (c); D units are shown in red, A units are shown in blue, hydrogen atoms and counter anions are omitted.

The transformation between homo-[2]-catenanes and MRs also could be observed *via* absorption spectra, as the strong π–π interaction leads to the narrowing of HOMO–LUMO gaps and remarkable red-shifts in absorption. As shown in Fig. S34,‡ the absorption of MR **1** in methanol solution (0.5 mM) is mainly in the ultraviolet and blue-light region (<500 nm). Upon formation of the interlocked structure (**Homo-1**), the absorption in the visible light region was significantly enhanced (500–700 nm). This type of red-shift effect caused by π–π interactions can be more clearly observed in the case of **Homo-2**, the absorption region of which extends to the NIR region (Fig. S35‡).

Heterogeneous [2]catenanes

In an attempt to further enhance the NIR absorption, we attempted to prepare mixed D–A stacking modes by hierarchical self-assembly. According to the conventional understanding of D–A interactions, the most favorable parallel arrangement of π-rich and π-deficient units is the D–A–D–A stacking pattern, containing a 1 : 1 ratio of π-rich and π-deficient units. Thus, we initially stirred a 1 : 1 mixture (8.0 mM) of **Homo-1** and **Homo-2** in an NMR tube with CD_3OD for 12 h at room temperature. A range of new signals were observed in the ^{1}H NMR spectrum, indicating the formation of a new compound (Fig. S17 and S18‡). However, the new signals were very crowded and difficult

to confidently assign. Moreover, all attempts to grow single crystals were unsuccessful. Four stacking modes potentially exist in such a dimer, including the conventional D–A–D–A, and unconventional D–A–A–D, A–D–D–A and D–D–A–A modes, which cannot be distinguished by NMR alone. However, when the ratio of π-rich and π-deficient units is changed as 3 : 1 or 1 : 3, the possible stacking modes would be reduced from four to two. So, we decided to adjust the feed ratio for reducing isomers.

We initially changed the feed ratio from 1 : 1 to 3 : 1 by stirring a 3 : 1 mixture (8.0 mM) of **Homo-1** and **Homo-2** in an NMR tube under the same conditions as described above (Fig. 2a). After 10 min, signals for **Homo-1**, MR **1**, **Homo-2** and MR **2** could be clearly observed in the ^{1}H NMR spectrum (Fig. 3, S19 and S20‡). After 12 h, we observed a range of new signals (Fig. 3). Although the new signals were highly complex because of low symmetry, DOSY NMR confirmed that they possessed the same diffusion coefficient (Fig. S21 and S22‡), indicating the formation of a new compound, denoted **Hetero-3**. According to the relative intensity of the signals of the benzoquinone unit, the proportion of **Hetero-3** in 8.0 mM methanol solution exceeded 75%. Thanks to the high proportion of **Hetero-3** in solution, we were able to grow single crystals of **Hetero-3**. As expected, a single-crystal X-ray crystallographic analysis confirmed the hetero-[2]catenanes structure of **Hetero-3** and established its unusual D–A–D–D stack (Fig. 2b), which further proved by ESI-MS (Fig. S32‡). Due to its mixed D–A stacking mode, the absorption of **Hetero-3** was further shifted to the low-energy region and extended into the NIR region, in marked contrast to the absorption profile of **Homo-1** (Fig. S34‡). This observation suggested that the mixed D–A stacking mode in metalla[2]catenanes may be an effective means to improve absorption in the NIR region.

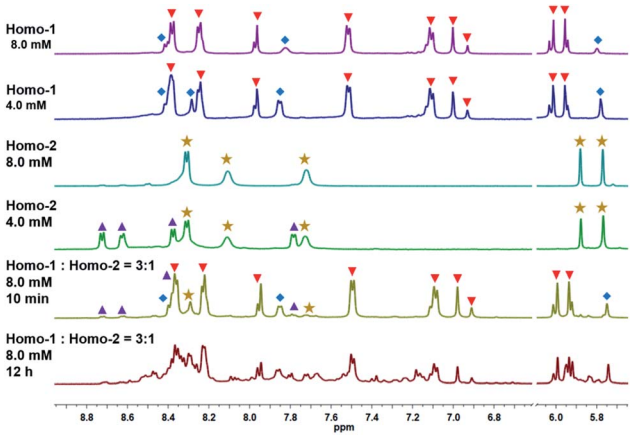

Fig. 3 Partial ^{1}H NMR spectrum of **Homo-1** (▼) + **1** (◆) (CD_3OD, 8.0 mM), **Homo-1** (▼) + **1** (◆) (CD_3OD, 4.0 mM), **Homo-2** (★) + **2** (▲) (CD_3OD, 8.0 mM), **Homo-2** (★) + **2** (▲) (CD_3OD, 4.0 mM), **Homo-1** + **Homo-2** (the ratio of **Homo-1** : **Homo-2** is 3 : 1, 10 min) (CD_3OD, 8.0 mM) and **Homo-1** + **Homo-2** (the ratio of **Homo-1** : **Homo-2** is 3 : 1, 12 h) (CD_3OD, 8.0 mM).

Following these results, we attempted to prepare the corresponding hetero-[2]catenanes with a mixed A–D–A–A stack

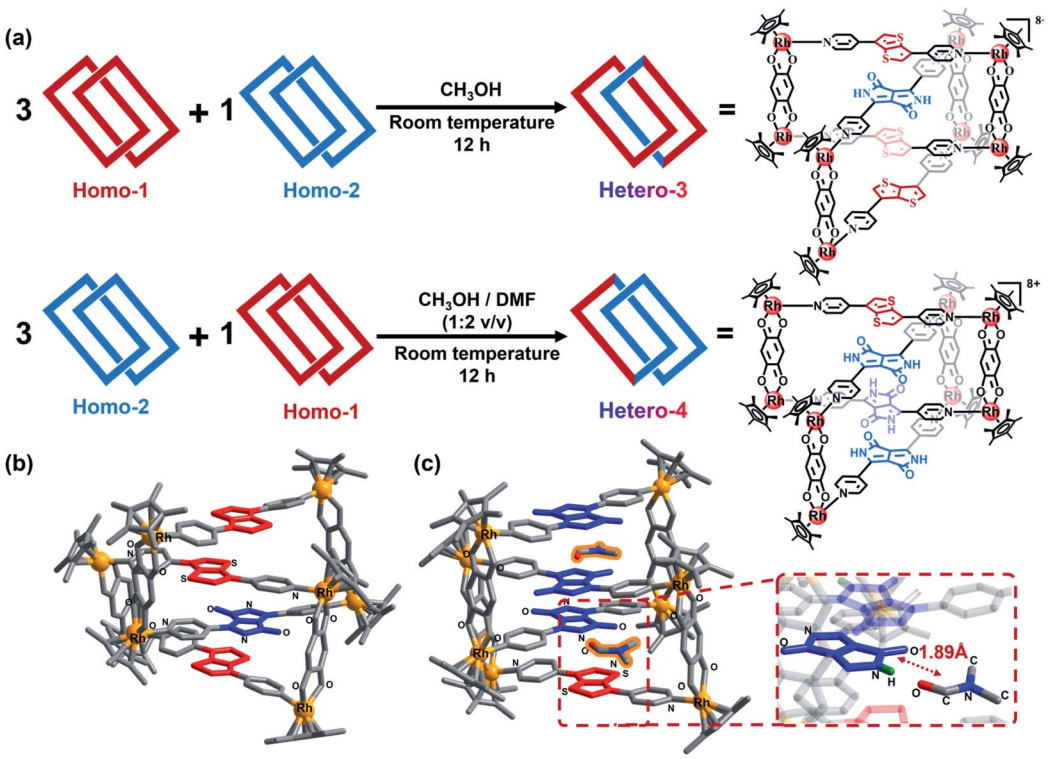

Fig. 2 (a) Hierarchical self-assembly for the synthesis of heterogeneous D–A metalla[2]catenanes; single-crystal X-ray structures of **Hetero-3** (b) and **Hetero-4** (c); the DMF molecule is highlighted with an orange glow, the D-unit is shown in red and the A-unit is shown in blue, the inset is hydrogen bond in **Hetero-4**, H atoms are shown in green, other hydrogen atoms and counter anions are omitted.

through a similar method. We thus adjusted the feed ratio by using a 1 : 3 mixture (8.0 mM) of **Homo-1** and **Homo-2**. However, to our disappointment, no obvious change was observed in ^{1}H spectrum even after three days (Fig. S23 and S24‡). Despite this result, we attempted to crystallize this mixture. In our experience, DMF improve the solubility of assemblies, and assist the growth of single crystals during crystallization.[13] Hence, similar to the experiments described above, DMF was added to the solution. To our surprise, black block single crystals appeared in the bottom of the tube after two weeks. A single-crystal X-ray crystallographic analysis established the new compound **Hetero-4** to also have a hetero-[2]catenanes structure, with a D/A ratio of 1 : 3, which confirmed by ESI-MS (Fig. S33‡). Moreover, the stacking mode of **Hetero-4** was not the expected A–D–A–A arrangement, but an unprecedented D–A–A–A form (Fig. 2c). This assembly can be attributed to the presence of DMF, as obvious hydrogen bonding interactions exist between the N–H groups of the A units and the oxygen atom of DMF, with distances of only *ca.* 1.89 Å (Fig. 2c). We also observed CH$\cdots\pi$ interactions between the H atoms of the DMF and the pyridyl group of certain pyridyl ligands (Fig. S37‡). The DMF molecules (highlighted in orange in Fig. 2c) act like nails that staple two metallarectangles together and allow formation of the abnormal D–A [2]catenanes. To further confirm the effect of DMF, we gradually added d_7-DMF to a solution of the **Homo-1**/**Homo-2** mixture. In ^{1}H NMR spectrum, some signals were found to grow gradually with increasing amounts of d_7-DMF (Fig. S25 and S26‡). A DOSY NMR spectrum showed that the growing signals have the same diffusion coefficient (Fig. S27‡). According to the relative intensity of the benzoquinone signal, the proportion of **Hetero-4** in an 8.0 mM CD_3OD/d_7-DMF (1 : 2 v/v) solution was *ca.* 80%. Moreover, **Hetero-4** displayed stronger NIR absorption (650–750 nm) than **Hetero-3** due to its higher proportion of diketo-pyrrolopyrrole groups (Fig. S35‡).

NIR photothermal conversion

Due to their strong NIR absorption, these D–A metalla[2]catenanes were found to have fascinating photothermal conversion properties. Under 730 nm laser irradiation (0.5 W cm^{-2}) for 250 s, the temperature of **Hetero-4** and **Hetero-3** sharply increased, reaching temperatures as high as 70 °C and 55 °C, respectively, markedly higher than those of **Homo-2** (45 °C) and **Homo-1** (37 °C) under the same conditions (Fig. 4a). The NIR-photothermal effect of crystals of **Hetero-4** upon exposure to a 730 nm laser can also be clearly observed from Fig. 4c. The cooling curve of **Hetero-4** is shown in Fig. S36,‡ from which the photothermal conversion efficiency was calculated (details are shown in ESI‡) to be 27.3%, which is better than the reported organic D–A cocrystal materials.[7a] This enhanced photothermal temperature and the higher photothermal conversion of heterogeneous metalla[2]catenanes can be attributed to the mixed D–A stacking mode and the fluorescence quenching effect from Cp*Rh fragments. In contrast to cocrystal materials, D–A metalla[2]catenanes still display satisfactory photothermal conversion properties in dissolved solution.[7a] As shown in Fig. 4b and d, under the same irradiation condition (300 s), the temperature of **Hetero-3** in 8.0 mM methanol solution and **Hetero-4** in 8.0 mM CH_3OH/DMF (1 : 2 v/v) reach maxima at 49 °C and 58 °C, respectively. As a contrast, physical mixtures of **L1** and **L2** (**L1** : **L2** = 3 : 1 or 1 : 3) in 8.0 mM DMSO solution experience temperature increases of only 2.5 °C and 3 °C under the same conditions (Fig. 4b). This results further confirm D–A metalla[2]catenanes as a promising platform for the development of NIR photothermal conversion materials.

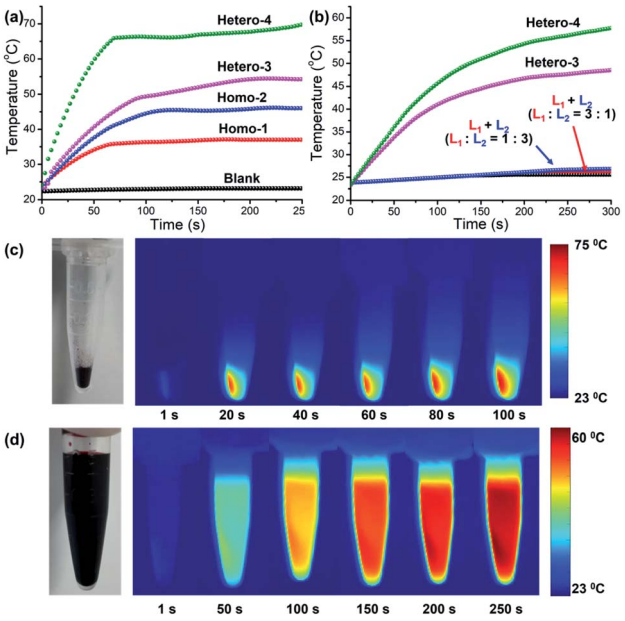

Fig. 4 (a) Photothermal conversion behavior of **Homo-1**, **Homo-2**, **Hetero-3** and **Hetero-4** (crystal) under 730 nm laser irradiation; (b) photothermal conversion behavior of **Hetero-3** in 8.0 mM methanol solution, **Hetero-4** in 8.0 mM CH_3OH/DMF (1 : 2 v/v) and the physical mixture of **L1** and **L2** (**L1** : **L2** = 3 : 1 or 1 : 3) in 8.0 mM DMSO solution under 730 nm laser irradiation; IR thermal images of **Hetero-4** crystals (c) and in 8.0 mM CD_3OD/d_7-DMF (1 : 2 v/v) (d) under 730 nm laser irradiation.

Conclusions

Hierarchical self-assembly has inherent advantages for the design of heterogeneous interlocked structures. We have employed an hierarchical self-assembly strategy to engineer heterogeneous D–A metalla[2]catenanes, leading to unconventional mixed D–A–D–D and D–A–A–A stacks in metalla[2]catenanes. Benefiting from the mixed D–A stacking modes and the fluorescence quenching effect from Cp*Rh fragments, heterogeneous D–A metalla[2]catenanes displayed high-performance NIR absorption and NIR photothermal conversion properties in crystalline and solution states. These results will not only allow chemists to design and synthesize complex structures that were previously inaccessible, but also provide promising candidates for materials science applications.

Conflicts of interest

There are no conflicts to declare.

Acknowledgements

This work was supported by the National Science Foundation of China (21531002, 21720102004, 21801045, 22031003) and the Shanghai Science and Technology Committee (19DZ2270100).

Notes and references

1 (*a*) R. S. Forgan, J. P. Sauvage and J. F. Stoddart, *Chem. Rev.*, 2011, **111**, 5434–5464; (*b*) G. Gil-Ramirez, D. A. Leigh and A. J. Stephens, *Angew. Chem., Int. Ed.*, 2015, **54**, 6110–6150; (*c*) S. Kassem, T. van Leeuwen, A. S. Lubbe, M. R. Wilson, B. L. Feringa and D. A. Leigh, *Chem. Soc. Rev.*, 2017, **46**, 2592–2621; (*d*) J. D. Crowley, S. M. Goldup, A. L. Lee, D. A. Leigh and R. T. McBurney, *Chem. Soc. Rev.*, 2009, **38**, 1530–1541; (*e*) J. R. J. Maynard and S. M. Goldup, *Chem*, 2020, **6**, 914–1932; (*f*) W. X. Gao, H. J. Feng, B. B. Guo, Y. Lu and G. X. Jin, *Chem. Rev.*, 2020, **120**, 6288–6325; (*g*) S. L. Huang, T. S. A. Hor and G. X. Jin, *Coord. Chem. Rev.*, 2017, **333**, 1–26.

2 (*a*) J. F. Stoddart and H. R. Tseng, *Proc. Natl. Acad. Sci. U. S. A.*, 2002, **99**, 4797–4800; (*b*) P. R. Ashton, T. T. Goodnow, A. E. Kaifer, M. V. Reddington, A. M. Z. Slawin, N. Spencer, J. F. Stoddart, C. Vicent and D. J. Williams, *Angew. Chem., Int. Ed. Engl.*, 1989, **28**, 1396–1399; (*c*) D. G. Hamilton, J. K. M. Sanders, J. E. Davies, W. Clegg and S. J. Teat, *Chem. Commun.*, 1997, 897–898; (*d*) K. Kitajima, T. Ogoshi and T. Yamagishi, *Chem. Commun.*, 2014, **50**, 2925–2927.

3 (*a*) A. C. Fahrenbach, C. J. Bruns, H. Li, A. Trabolsi, A. Coskun and J. F. Stoddart, *Acc. Chem. Res.*, 2014, **47**, 482–493; (*b*) J. M. Lehn, *Supramolecular Chemistry. Concepts and Perspectives*, Wiley-VCH, Weinheim, Germany, 1995.

4 (*a*) P. T. Corbett, J. Leclaire, L. Vial, K. R. West, J. L. Wietor, J. K. M. Sanders and S. Otto, *Chem. Rev.*, 2006, **106**, 3652–3711; (*b*) F. B. L. Cougnon, H. Y. Au-Yeung, G. D. Pantos and J. K. M. Sanders, *J. Am. Chem. Soc.*, 2011, **133**, 3198–3207; (*c*) H. Y. Au-Yeung, G. D. Pantos and J. K. M. Sanders, *J. Am. Chem. Soc.*, 2009, **131**, 16030–16031; (*d*) H. Y. Au-Yeung, G. D. Pantos and J. K. M. Sanders, *Angew. Chem., Int. Ed.*, 2010, **49**, 5331–5334; (*e*) H. Y. Au-Yeung, G. D. Pantos and J. K. M. Sanders, *J. Org. Chem.*, 2011, **76**, 1257–1268.

5 (*a*) M. Fujita, J. Yazaki and K. Ogura, *J. Am. Chem. Soc.*, 1990, **112**, 5645–5647; (*b*) W. L. Shan, Y. J. Lin, F. E. Hahn and G. X. Jin, *Angew. Chem., Int. Ed.*, 2019, **58**, 5882–5886; (*c*) H. Lee, P. Elumalai, N. Singh, H. Kim, S. U. Lee and K. W. Chi, *J. Am. Chem. Soc.*, 2015, **137**, 4674–4677; (*d*) S. A. Boer, R. P. Cox, M. J. Beards, H. X. Wang, W. A. Donald, T. D. M. Bell and D. R. Turner, *Chem. Commun.*, 2019, **55**, 663–666; (*e*) Y. Lu, D. Liu, Y. J. Lin, Z. H. Li and G. X. Jin, *Natl. Sci. Rev.*, 2020, DOI: 10.1093/nsr/nwaa164; (*f*) M. M. Siddiqui, R. Saha and P. S. Mukherjee, *Inorg. Chem.*, 2019, **58**, 4491–4499; (*g*) Y. W. Zhang, S. Bai, Y. Y. Wang and Y. F. Han, *J. Am. Chem. Soc.*, 2020, **142**, 13614–13621; (*h*) T. Feng, X. Li, Y. Y. An, S. Bai, L. Y. Sun, Y. Li, Y. Y. Wang and Y. F. Han, *Angew. Chem., Int. Ed. Engl.*, 2020, **59**, 13516–13520; (*i*) S. Mukherjee and P. S. Mukherjee, *Chem. Commun.*, 2014, **50**, 2239–2248.

6 (*a*) Y. J. Liu, P. Bhattarai, Z. F. Dai and X. Y. Chen, *Chem. Soc. Rev.*, 2019, **48**, 2053–2108; (*b*) K. K. Ng and G. Zheng, *Chem. Rev.*, 2015, **115**, 11012–11042; (*c*) Y. Y. Li, J. Wang, F. Zhao, B. Bai, G. J. Nie, A. E. Nel and Y. L. Zhao, *Natl. Sci. Rev.*, 2018, **5**, 365–388.

7 (*a*) Y. Wang, W. G. Zhu, W. N. Du, X. F. Liu, X. T. Zhang, H. L. Dong and W. P. Hu, *Angew. Chem., Int. Ed.*, 2018, **57**, 3963–3967; (*b*) Q. Song, Y. Jiao, Z. Q. Wang and X. Zhang, *Small*, 2016, **12**, 24–31; (*c*) A. Das and S. Ghosh, *Angew. Chem., Int. Ed.*, 2014, **53**, 2038–2054.

8 (*a*) Y. Lu, H. N. Zhang and G. X. Jin, *Acc. Chem. Res.*, 2018, **51**, 2148–2158; (*b*) Y. Lu, Y. X. Deng, Y. J. Lin, Y. F. Han, L. H. Weng, Z. H. Li and G. X. Jin, *Chem*, 2017, **3**, 110–121.

9 (*a*) V. Vajpayee, Y. H. Song, T. R. Cook, H. Kim, Y. Lee, P. J. Stang and K. W. Chi, *J. Am. Chem. Soc.*, 2011, **133**, 19646–19649; (*b*) Y. F. Han and G. X. Jin, *Acc. Chem. Res.*, 2014, **47**, 3571–3579.

10 M. Kaur and D. H. Choi, *Chem. Soc. Rev.*, 2015, **44**, 58–77.

11 S. Datta, M. L. Saha and P. J. Stang, *Acc. Chem. Res.*, 2018, **51**, 2047–2063.

12 (*a*) W. M. Bloch, J. J. Holstein, B. Dittrich, W. Hiller and G. H. Clever, *Angew. Chem., Int. Ed.*, 2018, **57**, 5534–5538; (*b*) X. Z. Yan, T. R. Cook, J. B. Pollock, P. F. Wei, Y. Y. Zhang, Y. H. Yu, F. H. Huang and P. J. Stang, *J. Am. Chem. Soc.*, 2014, **136**, 4460–4463; (*c*) R. F. Wen, S. S. Xu, D. L. Zhao, L. X. Yang, X. H. Ma, W. Liu, Y. C. Lee and R. G. Yang, *Natl. Sci. Rev.*, 2018, **5**, 878–887.

13 Y. Lu, Y. J. Lin, Z. H. Li and G. X. Jin, *Chin. J. Chem.*, 2018, **36**, 106–111.